
Article:
Chen, L, Ettelaie, R orcid.org/0000-0002-6970-4650 and Akhtar, M (2019) Improved enzymatic accessibility of peanut protein isolate pre-treated using thermosonication. Food Hydrocolloids, 93. pp. 308-316. ISSN 0268-005X

https://doi.org/10.1016/j.foodhyd.2019.02.050

Accepted Manuscript

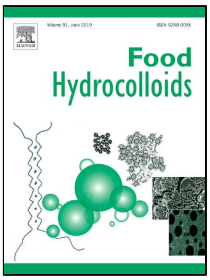

Improved enzymatic accessibility of peanut protein isolate pre-treated using thermosonication

Lin Chen, Rammile Ettelaie, Mahmood Akhtar

PII:	S0268-005X(18)32168-4
DOI:	10.1016/j.foodhyd.2019.02.050
Reference:	FOOHYD 4976
To appear in:	*Food Hydrocolloids*
Received Date:	05 November 2018
Accepted Date:	25 February 2019

Please cite this article as: Lin Chen, Rammile Ettelaie, Mahmood Akhtar, Improved enzymatic accessibility of peanut protein isolate pre-treated using thermosonication, *Food Hydrocolloids* (2019), doi: 10.1016/j.foodhyd.2019.02.050

Improved enzymatic accessibility of peanut protein isolate pre-treated using thermosonication

Lin Chen [a,*], Rammile Ettelaie [b], Mahmood Akhtar [b]

[a] *School of Chemical Engineering and Light Industry, Guangdong University of Technology, Guangzhou 510006, China*

[b] *Food Colloids Groups, School of Food Science and Nutrition, University of Leeds, Leeds LS2 9JT, UK*

* corresponding author: Dr. Lin Chen

Tel/Fax: +86-20-39322203

E-mail: l.chen@gdut.edu.cn

6 Figures

5 Tables

Abstract

Thermosonication pre-treatment was used to enhance the pancreatin-induced proteolysis of peanut protein isolate (PPI). Response surface methodology was applied to optimize the thermosonication conditions (including power-output and temperature), and the highest degree of hydrolysis (7.16%) was obtained at 475.0 W, 72 °C. SDS-PAGE analysis showed that at this optimized condition, the enzymatic accessibility of the major constitutive protein arachin in thermosonicated PPI (TS-PPI) was substantially improved compared to that in untreated PPI or sonicated PPI (475 W, 30°C; S-PPI), resulting in a remarkable increase in protein solubility for the hydrolysates. Protein denaturation and conformation profiles of untreated PPI, S-PPI and TS-PPI were investigated using differential scanning calorimetry, intrinsic fluorescence emission spectroscopy, Fourier transform infra-red spectroscopy and thioflavin-T (ThT) fluorescence assay. It was found that heat could present a markedly additive effect to ultrasound on denaturing peanut proteins, leading to significant changes in protein conformation. TS-PPI was characterized by the appearance of high proportion of parallel intermolecular β-sheets and a strong fluorescence enhancement upon binding to ThT, suggesting that the protein unfolding and aggregation induced by thermosonication probably resulted in the formation of fibril protein aggregates in TS-PPI rather than spherical protein aggregates formed in S-PPI. As a result, the protein conformation of TS-PPI appeared to be more unfolded and flexible than that of untreated PPI or S-PPI, and therefore was more easily accessible to protease. This study shows that thermosonication pre-treatment could be a highly effective and feasible technique to improve the enzymatic accessibility of globular proteins, producing prominent functional benefits for the protein hydrolysates.

Keywords: peanut protein isolate; thermosonication pre-treatment; enzymatic accessibility; protein denaturation; protein aggregation

1. Introduction

Peanut is a particularly valuable source of protein that have high biological values, desirable functionalities and relatively low cost (Ghatak & Sen, 2013; Zhao, Chen, & Du, 2012). Peanut protein isolate (PPI) is the most refined peanut protein product, containing ca. 90% protein on dry weight basis, and has been used in a wide range of food application, including vegetarian sausages, nutritional beverages, and dairy product replacements (Zhao et al., 2012). The current popularity of peanut protein-based food continues to drive PPI research and commercial development. Exploring effective PPI modification techniques leading to improved processing and nutritional characteristics will facilitate its use in the production of protein-based foods with improved quality.

Enzymatic proteolysis, which utilizes protease to catalyze the hydrolysis of peptide bonds under mild conditions, converts proteins into peptides of various sizes and free amino acids. The enzymatic hydrolysis of food proteins offers a possibility to obtain hydrolysates with improved functional properties (Tavano, 2013; Zeeb, McClements, & Weiss, 2017). Also, enzyme-hydrolyzed food proteins including PPI have been reported to have biologically active properties, such as anti-oxidant and anti-hypertensive effects (Jamdar et al., 2010; Li et al., 2011). Usually, enzymatic processes are highly efficient and safe for proteolysis. However, previous studies have found that PPI is generally resistant to enzymatic proteolysis, because its major constitutive proteins arachin and conarachin have compact globular structures that protect many of the peptide bonds (Chen, Chen, Yu, Wu, & Zhao, 2018; Perrot, Quillien, & Guéguen, 1999; Zhao, Liu, Zhao, Ren, & Yang, 2011). With this regard, attempts should be made to alter the structural characteristics of PPI in order to increase its enzymatic accessibility, which has been proven to be of key importance on achieving desirable functionalities for the final protein hydrolysates (Chen, Chen, Yu, & Wu, 2016; Chen et al., 2018; Zeeb et al., 2017).

Thermosonication is a novel food processing technique that utilizes power ultrasound in combination with mild heating (T > 50 ºC) (Chandrapala, Oliver, Kentish, & Ashokkumar, 2012; Patist & Bates, 2008). Recently, several studies have reported that compared to sonication alone, thermosonication appears to be more effective in denaturing proteins (Baltacıoğlu, Bayındırl, & Severcan, 2017; Villamiel & de Jong, 2000), inactivating enzymes (Ribeiro, Valdramidis, Nunes, & de Souza, 2017), or disrupting protein particles (Gordon & Pilosof, 2010). For example, Villamiel and de Jong (2000) reported that a synergism existed between the denaturing effect of ultrasound and heat on α-lactalbumin and β-lactoglobulin. Baltacıoğlu et al. (2017) found that no significant change ($p > 0.05$) in the secondary structure composition of polyphenol oxidase could be detected when sonication (24 kHz, 400 W, 10 min) was conducted at 20 ºC; however, the structural changes became evident when the same sonication was conducted at 60 ºC. This may be due to the fact that the effects of ultrasound on liquid systems are mainly related to the cavitation phenomenon, and the temperature of sonicated medium is one of the most important parameters that affects the behavior of cavitation bubbles (Chandrapala et al., 2012; Patist & Bates, 2008). According to the cavitation physics, increasing the temperature during sonication allows a reduction in cavitation threshold, so that more cavitation bubbles are produced, leading to more heat-generating bubble movements and collapses, and this could provide a more uniform and intense acoustic filed. However, as the temperature rises, liquid has higher vapor pressure inside the bubbles, which poses a cushioning effect against the implosion force of inertial cavitation, thus reducing cavitation intensity (Ashokkumar, Lee, Kentish, & Grieser, 2007; Patist & Bates, 2008). These two opposing tendencies suggest that an optimal temperature might occur at which the acoustic cavitation is more intensive or more effective for the desirable modifications (Baltacıoğlu et al., 2017; Gordon & Pilosof, 2010; Patist & Bates, 2008;

Ribeiro et al., 2017; Villamiel & de Jong, 2000). It has been demonstrated that thermosonication could alter the structure of globular proteins, resulting in the exposure of inner groups previously buried, and therefore has the potential to alter the enzymatic accessibility of PPI. However, current studies have not elucidated the possible synergistic, additive or antagonistic effect of temperature and ultrasound on the enzymatic proteolysis of PPI and there is a need to optimize such processes in relation to the processing conditions.

The enzymatic accessibility of proteins is closely correlated to their molecular conformation (Tavano, 2013; Zeeb et al., 2017). Furthermore, the changes in protein conformation results from specific molecular changes occurring as denaturation and aggregation progress (Belloque, Chicón, & López-Fandiño, 2007; Lefèvre & Subirade, 2000; Nyemb et al., 2014). For a better knowledge on how thermosonication pre-treatment could enhance the enzymatic proteolysis of PPI, it is of great interest to understand the molecular differences of denaturation/aggregation that lead to the formation of protein samples with different enzymatic accessibilities. However, to our knowledge, a limited research on the topic has been reported in the literature. Therefore, this study aims to optimize the effect of thermosonication pre-treatment conditions (including ultrasound power-output and temperature) on the enzymatic proteolysis of PPI using response surface methodology (RSM). Furthermore, by investigating some key changes in protein conformation of PPI caused by thermosonication, it is hoped that the underpinning mechanism of improved enzymatic accessibility for TS-PPI can be more clearly understood.

2. Materials and methods

2.1. Materials

PPI was prepared from low-temperature defatted peanut meal (Tianshen Bioprotein Co. Ltd.,

Taixing, China) according to the method of Zhao et al. (2011), with slight modifications. Briefly, the PPI was prepared using alkaline extraction (pH = 8.0) followed by precipitation using the isoelectric pH condition of peanut protein (p*I*, 4.5); the precipitated proteins were collected and re-suspended in deionized water, with the pH being adjusted to pH 7.0; the resultant dispersion was then lyophilized, finely milled, and kept in sealed plastic bottles. The protein content of this prepared PPI was 88.6 g/100 g of powder, determined by Kjeldahl method (N × 5.46). Pancreatin (8× standard USP unit) and phenylmethanesulfonyl fluoride (PMSF) were purchased from Sigma Chemicals (St. Louis, MO, USA). Laemmli sample buffer, Tris-HCl precast gel (4–15 %), β-mercaptoethanol, and Coomassie Brilliant Blue R-250 were purchased from Bio-Rad Laboratories (Hercules, CA, USA). All other chemicals used were at least of analytical grade. Water purified with a Milli-Q filtration unit (Millipore, Bedford, UK) was used for the preparation of solutions or sample dispersions. HCl (0.1–1.0 mol/L) and NaOH solutions (0.1–1.0 mol/L) were used for pH adjustment.

2.2. Thermosonication pre-treatment of PPI

PPI dispersions (50 g/L) were magnetically stirred at room temperature (21 ± 2 ºC) for 2 h to ensure complete hydration, with pH being adjusted to 7.0. The thermosonication pre-treatment on PPI dispersions was conducted using a laboratory-type ultrasound processor (Zhenyuan Ultrasonic Electron Equipment Co. Ltd, Hangzhou, China), model ZYS20-1000 (0–500 W, 24 kHz, 120 μm at 100 % amplitude), equipped with a digital power-output regulator, a digital timer, a temperature controller, and a titanium sonotrode (22 mm in diameter). PPI dispersions (250 mL) were heated in a water bath to achieve desired temperatures and transferred to a double-walled beaker (inner diameter: 8 cm, depth: 13.5 cm) with a cooling/heating system. The sonotrode was immersed about 30 mm into the PPI dispersions, and was sonicated for 100 cycles, where each cycle consisted of 5 s ultrasound pulse on

127 and 1 s off. A magnetic stirrer was used to assure the homogeneity of the dispersions. The temperature
128 of PPI dispersions was controlled with a peristaltic pump (working at 7.5 L/min) connected to a
129 temperature-controlled water bath, which could ensure that sample dispersions remained within ± 2 ºC
130 of a set temperature. Immediately after the time schedule, the samples were cooled down in an ice-
131 water bath. Finally, the dispersions of thermosonicated PPI (TS-PPI) were lyophilized, finely milled,
132 and kept at 4 ºC in sealed plastic bottles for further use. Several experiments were performed at a
133 temperature of 30 ºC (± 2 ºC) to study the effect of ultrasound without the influence of heat treatment
134 and the resultant sample was referred to sonicated PPI (S-PPI).

135 **2.3. Enzymatic proteolysis and degree of hydrolysis (DH) determination**

136 To identify the exposed hydrolysis sites of PPI after thermosonication pre-treatment as much as
137 possible, the enzymatic proteolysis was induced using pancreatin, which has a very broad specificity to
138 peptide bonds and preferentially cleaves hydrophobic residues (Adler-Nissen, 1986). Fully hydrated
139 sample dispersions (50 g/L, pH 7.0) were prepared using deionized water as described above and were
140 pre-incubated at 50 ºC for 15 min before proteolysis. Pancreatin was then added into the sample
141 dispersions to a protease-to-substrate ratio of 0.5% w/w, and the enzymatic proteolysis was conducted
142 at 50 ºC and pH 7.0 in a temperature-controlled shaking water bath operating at 120 rpm. During the
143 enzymatic proteolysis, the pH of sample dispersions was maintained using an auto-titrator (848 Titrino
144 plus, Metrohm, Switzerland) loaded with 0.1–1.0 mol/L NaOH solutions. Based on the preliminary
145 experiments, the proteolysis time were set at 60 min, so that the enzymatic proteolysis for each
146 substrate/protease combination could reach a DH plateau. At the end of the proteolysis time, the
147 protease inhibitor PMSF was added into the sample dispersions to a concentration of 1 mmol/L so as
148 to terminate the pancreatin-induced proteolysis. The consumption of NaOH solution was recorded for

149 the determination of DH using pH-stat method (Adler-Nissen, 1986).

150 **2.4. Optimization of thermosonication pre-treatment conditions using response surface**
151 **methodology (RSM)**

152 The operating conditions of thermosonication pre-treatment were optimized using RSM with a
153 central composite design (CCD) in order to prepare TS-PPI hydrolysates (TS-PPIH) with high DH
154 values. Based on the preliminary experiments, the ultrasonic power-output (X_1) and the temperature
155 of sonicated medium (X_2) were chosen as independent variables, which were found to have
156 pronounced influence on the DH (Y_0) of TS-PPIH. The experimental design consisted of 13 factorial
157 experiments with 5 replicates of the central point. The coded and actual levels of the two variables
158 are shown in **Table 1**. The software Design-Expert (Version 8.0.6, Stat-Ease Inc., Minneapolis, Minn.,
159 USA) was used for experimental design, data analysis, and model building. The full experimental
160 design with respect to real values of the independent variables, and the attained experimental values
161 and predicted values of the response (DH) are presented in **Table 2**. Data were then analyzed using
162 the least squares method to fit the following second-order polynomial model equation:

163 $$Y_0 = b_0 + \sum_{i=1}^{k} b_i X_i + \sum_{i=1}^{k} b_{ii} X_i^2 + \sum_{i=1}^{k-1} \sum_{j>1}^{k} b_{ij} X_i X_j$$

164 where Y_0 is the predicted response variable, X_i and X_j are independent variables, and k is the number
165 of tested variables (k = 2). The regression coefficient is defined as b_0 for the intercept, b_i for linear,
166 b_{ii} for quadratic and b_{ij} for interaction terms. Analysis of variance (ANOVA) was performed to
167 determine the significance of the model. The fitness of the model was examined in terms of coefficient
168 of determination (R^2), adjusted-R^2, and predicted-R^2.

169 **2.5. Determination of protein solubility (PS)**

170 The PS of different protein samples were determined according to the method described in our

171 previous research (Chen et al., 2016). Briefly, fully hydrated sample dispersions (10 g/L, pH 7.0)
172 were prepared using deionized water as described above. The resulting dispersions were centrifuged
173 at 12,000 *g* for 30 min to collect supernatants. The soluble nitrogen content in supernatants was
174 determined by the Kjeldahl method, and the PS was expressed as a percentage of soluble nitrogen in
175 the supernatant against total nitrogen presented in the sample.

176 **2.6. Sodium dodecyl sulphate-polyacrylamide gel electrophoresis (SDS-PAGE)**

177 SDS-PAGE was conducted under reducing conditions using the Laemmli method (Laemmli,
178 1970), with slight modifications. Briefly, 100 μL of fully hydrated sample dispersions (20 g/L, pH
179 7.0) was mixed with 100 μL of Laemmli sample buffer (containing 10 μL of β-mercaptoethanol). The
180 mixtures were heated at 95 °C for 10 min and were then centrifuged at 10,000 *g* for 5 min. Aliquot
181 (15 μL) of each sample was loaded onto the Tris-HCl precast gradient gel (4–15 %) for electrophoresis
182 running in a Mini-protean Tetra system (Bio-Rad Laboratories). Electrophoresis was conducted at
183 200V until the indicator dye reached the bottom of the gel. After separation, proteins were fixed and
184 stained using Coomassie Brilliant Blue R-250.

185 **2.7. Differential scanning calorimetry (DSC)**

186 DSC measurements were performed to investigate the thermal properties of protein samples
187 using a TA Q100-DSC thermal analyzer (TA Instruments, New Castle, DE). Fully hydrated sample
188 dispersions (100 g/L, pH 7.0) were prepared using 0.01 mol/L phosphate buffer as described above.
189 Aliquot (10 μL) of the resulting dispersion was precisely injected into an aluminum pan. The pan was
190 then hermetically sealed and was heated in the calorimeter from 20 to 120 ºC at a rate of 5 ºC/min. A
191 sealed empty pan was used as the reference. The denaturation parameters were calculated from the
192 thermograms by the Universal Analyzer 2000 software (version 4.1D, TA Instrument): the

193 denaturation temperature (T_d) was considered as the value corresponding to the maximum transition
194 peak, and the transition enthalpy (ΔH) was calculated from the area below the transition peak.

195 **2.8. Intrinsic fluorescence emission spectroscopy**

196 The intrinsic fluorescence emission spectra of tryptophan (Trp) residues in protein samples
197 were measured using a RF-5301 fluorophotometer (Shimadzu Co., Kyoto, Japan). Fully hydrated
198 sample dispersions (15 g/L, pH 7.0) were prepared using 0.01 mol/L phosphate buffer. To minimize
199 the contribution of tyrosine residues to the emission spectra, sample dispersions were excited at 290
200 nm. The emission spectra were recorded from 300 to 400 nm at a constant slit of 5 nm.

201 **2.9. Fourier transform infra-Red (FTIR) spectroscopy**

202 The preparation and FTIR analysis of protein samples were performed according to the method
203 of Baltacıoğlu et al. (2017), with slight modifications. Sample dispersions (50 g/L) were prepared
204 using deuterated phosphate buffer solution (0.01 mol/L, pD 7.0). D_2O instead of H_2O was used as a
205 solvent in FTIR analysis, because D_2O was proven to be of greater transparency in the infrared region
206 (1600–1700 cm^{-1}) compared to H_2O. To ensure complete D-H exchange, sample dispersions were
207 gently stirred at 4 °C for 24 h. Infrared spectra of dispersions of protein samples were recorded using
208 a Nicolet iS50 FTIR spectrometer (Thermo Nicolet Co., Madison, WI, USA), equipped with an
209 attenuated total reflection (ATR) accessory. Samples were held in an IR cell and were recorded
210 against D_2O background in absorbance mode from 4000 to 400 cm^{-1}. A total of 32 scans were
211 averaged at 4 cm^{-1} resolution. Protein secondary structure prediction was based on a combination of
212 Fourier self-deconvolution with a band-fitting procedure (Byler & Susi, 1986; Kong & Yu, 2007).
213 For the deconvolution, a half-bandwidth of 10.5 cm^{-1} and a resolution enhancement factor of 2 were
214 used. For the band-fitting, initial band frequencies were determined from the second derivatives of

215 the deconvoluted spectra. Deconvolution and second derivative of infrared spectra were both
216 performed using the Omnic software package (Version 8.0, Thermo Nicolet Co.). The areas of the
217 bands were calculated by integration of the corresponding fitted band and were used for quantitative
218 analysis of secondary structure components.

219 **2.10. Thioflavin-T fluorescence assay**

220 The thioflavin-T (ThT) fluorescence assay was performed according to the method of
221 Stathopulos et al. (2004), with slight modifications. ThT solution (3 mmol/L) was prepared by
222 dissolving ThT powder into phosphate buffer (0.01 mol/L, pH 7.0), and was filtered through a 0.2 μm
223 syringe filter to remove undissolved power. Fully hydrated sample dispersions (0.2 g/L, pH 7.0) were
224 prepared using the same phosphate buffer. Twenty microliters of ThT solution was added to 2.98 mL
225 aliquots of sample dispersions, and the fluorescence data of the resulting mixtures were measured
226 using a RF-5301 fluorophotometer (Shimadzu Co.). The mixtures were excited at 450 nm, and the
227 emission spectra were recorded from 400 to 600 nm at a constant slit of 5 nm. Spectra of samples
228 with no ThT were subtracted from the spectra for corresponding samples containing ThT.

229 **2.11. Statistical analysis**

230 Unless otherwise stated, all the tests were performed in triplicate. Results were subjected to
231 ANOVA. Duncan's multiple-range test was applied to identify significant differences between results
232 ($p < 0.05$) using SPSS 13.0 software (SPSS Inc., Chicago, IL, USA).

233 **3. Results and discussion**

234 **3.1. Effects of the power-output and temperature of thermosonication pre-treatment on the**
235 **DH of TS-PPIH**

236 The application of RSM yields the regression Eq. (1), which represents an empirical relationship

between the response (DH) and the tested variables, i.e. power-output (X_1) and temperature (X_2) of thermosonication pre-treatment:

$$\mathrm{DH} = -6.92 + 0.027X_1 + 0.22X_2 - 0.0001X_1X_2 - 0.000021X_1^2 - 0.0012X_2^2 \quad (1)$$

The fitted model equation has been analyzed by ANOVA and the results are shown in **Table 3**. It is seen that the model was highly significant ($p < 0.01$), the lack of fit was not significant ($p > 0.05$), and the R^2 value was determined to be 0.9887, indicating that the model equation developed adequately defined the true behavior of the system. The predicted-R^2 of 0.9520 was in reasonable agreement with the adjusted-R^2 of 0.9806, indicating a high degree of correlation between the experimental and the predicted values. All these results imply that the fitted model (Eq. 1) gave a satisfactory mathematical description on the effects of power-output and temperature of thermosonication pre-treatment on the DH of TS-PPIH.

As shown in **Table 3**, the ANOVA results showed significant ($p < 0.05$) linear (X_1 and X_2), interactive (X_1X_2) and quadratic (X_1^2 and X_2^2) effects on the response (DH). Based on the F-values of the regression coefficients, the linear term of ultrasonic power-output (X_1) revealed a major effect on the response, followed by X_2 (temperature), X_2^2, X_1^2, and X_1X_2. It is well-known that sonication causes various structural changes for proteins depending on ultrasonic power-output, because the ultrasonic power-output not only determines the imparted acoustic pressure in the medium, but also determines the acoustic pressure amplitude (controlled by ultrasonic wave amplitude), which has a strong influence on the acoustic cavitation activity (Chandrapala et al., 2012; Patist & Bates, 2008). The 3D response surface graph and binary contour plot, which were drawn to illustrate the effects of power-output and temperature of thermosonication pre-treatment on the DH of TS-PPIH, are shown in **Fig. 1a** and **b**, respectively. We can see that the DH increased gradually as the ultrasonic power-

259 output increased from 300 W to ca. 450–475 W, and then changed slightly thereafter. This tendency
260 was more apparent when the temperature was low. These results suggest that in order to effectively
261 enhance the enzymatic proteolysis of PPI, relatively high levels of power-output were required for
262 thermosonication pre-treatment, especially at low temperature. On the other hand, it is noteworthy
263 that at the same power-output level, the DH of TS-PPIH went up markedly with the temperature of
264 sonicated medium increasing from 50 ºC to ca. 70–75 ºC, but then decreased at higher temperature.
265 These results clearly indicated that in the certain temperature range, heat presented an additive effect
266 to ultrasound treatment on enhancing the enzymatic proteolysis of PPI. From the predictions of RSM
267 analysis, the optimal condition of thermosonication pre-treatment for maximizing the DH of TS-PPIH
268 was: power-output = 466.2 W, temperature = 71.7 °C, and the predicted DH was 7.08%. To confirm
269 the validity of this prediction, an approximate verification experiment was conducted. Taking the cost
270 and feasibility into account, the thermosonication condition was set to be: power-output = 475.0 W,
271 temperature = 72.0 °C, and the actual DH of TS-PPIH achieved was 7.16%, which was not
272 significantly different ($p > 0.05$) from the predicted DH. In the following studies, this optimized
273 thermosonication condition was used to prepare TS-PPI to investigate the changes in structural
274 properties of PPI in relation to its enzymatic accessibility.

275 **3.2. Effects of thermosonication pre-treatment on the enzymatic accessibility of PPI**

276 To investigate the effects of thermosonication pre-treatment on the enzymatic accessibility of
277 PPI, the SDS-PAGE profiles, DH and PS of untreated PPI, thermo-treated PPI (72 °C, 10 min; T-
278 PPI), sonicated PPI (475 W, 30°C, 100 cycles; S-PPI), thermosonicated PPI (475 W, 72°C, 100 cycles;
279 TS-PPI) and their hydrolysates (PPIH, T-PPIH, S-PPIH, and TS-PPIH) were investigated.

280 SDS-PAGE was performed to investigate the protein degradation in PPI caused by different

281 treatments. From **Fig. 2**, we can see that the electrophoretic profiles of tested PPI samples all
282 displayed five major bands, S66, S41, S40, S38, and S27, named by their molecular weights (MW).
283 Among them, Band S66 was identified as the subunit of conarachin, bands S41, S40, and S38 were
284 identified as the acidic subunits (AS) of arachin, and band S27 was identified as the basic subunit
285 (BS) of arachin (Chen et al., 2018; Ghatak & Sen, 2013; Zhao et al., 2011). However, in S-PPI and
286 TS-PPI, the band intensity of these subunits appeared to be weaker than that in untreated PPI, and
287 stained proteinaceous material that did not enter the gel was observed. These observations are
288 consistent with some previous studies, which showed that ultrasound treatment caused the formation
289 of protein aggregates that could not be broken down completely by SDS-reducing buffers (Jiang et
290 al., 2017; Stathopulos et al., 2004). After pancreatin-induced proteolysis, conarachin (S66) in PPIH
291 was degraded completely, while AS-arachin (S41–S38) and BS-arachin (S27) appeared to be almost
292 intact, suggesting that they were resistant to pancreatin-induced proteolysis. These observations are
293 similar to the observations from other researchers, which reported that arachin was located in the
294 inner part of peanut protein molecule and had a compact globular structure that was resistant to
295 enzymatic proteolysis (Chen et al., 2018; Perrot et al., 1999; Zhao et al., 2011). Compared with PPIH,
296 T-PPIH showed a similar electrophoretic pattern. As for S-PPIH, the band intensity of AS-arachin
297 decreased markedly, but BS-arachin was still clearly identifiable. In addition, one unanticipated
298 finding was that residual conarachin band (S66) was detected in S-PPIH, suggesting that the
299 enzymatic accessibility of conarachin was actually decreased after sonication pre-treatment. Again,
300 similar observations have been reported on the effects of thermal (Bax et al., 2012; Blayo, Vidcoq,
301 Lazennec, & Dumay, 2016) and high-pressure (Belloque et al., 2007; Sun, Mu, Sun, & Zhao, 2014)
302 on the enzymatic accessibility of globular proteins. It has been suggested that after physical pre-

303 treatments, the changes in the enzymatic accessibility of globular proteins are rather complex, and
304 closely related to the changes in protein conformation (Belloque et al., 2007; Blayo et al., 2016;
305 Nyemb et al., 2014).

306 By contrast, it was found that all the peanut protein subunits appeared to be readily hydrolyzed
307 after thermosonication pre-treatment, because they underwent total degradation in TS-PPIH. In
308 addtion, as shown in **Table 4**, the DH value of TS-PPIH (7.16%) was significantly ($p < 0.05$) higher
309 than those of PPIH (2.73%) or S-PPIH (3.84%), indicating that the combined use of heat and
310 ultrasound was more effective in improving the enzymatic accessibility of PPI than ultrasound
311 treatment alone. Furthermore, it is noteworthy that since all the subunits were degredated completely,
312 the TS-PPIH was mainly composed of peptides with MW < 20 kDa and showed a PS of 93.5%, much
313 higher than that of untreated PPI (PS = 74.8%). The high PS of TS-PPIH would be benefical for
314 utilizing peanut proteins in food products, such as protein beverages. These findings are encouraging
315 and suggest that the combined use of thermosonication and enzymatic proteolysis could be an
316 effective way to modify the functionality of globular proteins for specific applications.

317 **3.3. Effects of thermosonication pre-treatment on the conformation of PPI**

318 In attempt to explore the underpinning mechanisms of improved enzymatic accessibility for TS-
319 PPI, conformational differences between different protein samples were investigated by examining
320 their DSC thermograms, intrinsic and ThT fluorescence emission spectra, and FTIR spectra.

321 The DSC thermograms of different protein samples are shown in **Fig. 3**, and the calculated
322 denaturation parameters are summarized in **Table 4**. The DSC thermogram of untreated PPI showed
323 two major endothermic peaks at 85.9 °C and 105.3 °C, which corresponded to the thermal
324 denaturation temperature (T_d) of conarachin and arachin, respectively (Colombo, Ribtta, & León,

325 2010; Zhao et al., 2011). The transition enthalpy (ΔH) is positively correlated with the proportion of
326 undenatured protein (Colombo et al., 2010). Compared to untreated PPI, T-PPI showed a slight
327 decrease in the ΔH of both conarachin and arachin, suggesting that peanut proteins had a high thermal
328 stability, as also reported in the literature (Colombo et al., 2010; Ochoa-Rivas, Nava-Valdez, Serna-
329 Saldívar, & Chuck-Hernández, 2017); the S-PPI showed a marked decrease in the ΔH of conarachin
330 but only a slight decrease in that of arachin. Protein denaturation caused by ultrasound treatment is
331 mainly attributed to acoustic cavitation. Cavitation-induced activities, such as high local temperature,
332 shock waves, water jets and free radicals, could modify protein conformation by affecting hydrogen
333 bonds and hydrophobic interactions, disrupting protein quaternary and/or tertiary structures, and
334 therefore cause the denaturation of proteins (Baltacıoğlu et al., 2017; Stathopulos et al., 2004;
335 Villamiel & de Jong, 2000). The endothermic peaks of conarachin and arachin in the thermogram of
336 TS-PPI were almost disappeared and showed very low ΔH values, suggesting that peanut proteins
337 were almost wholly denatured by thermosonication conducted at 72 ºC. This finding agreed with
338 previous studies, which showed that heat could present a markedly additive effect to ultrasound
339 treatment on denaturing proteins, probably because the acoustic cavitation activity generated by
340 ultrasound was closely related to the temperature of sonicated medium (Ashokkumar et al., 2007;
341 Baltacıoğlu et al., 2017; Villamiel & de Jong, 2000). Contrasting the denaturation extent with
342 enzymatic accessibility for untreated PPI, S-PPI and TS-PPI, a positive correlation can be found
343 between the two parameters. However, the relationship between protein denaturation extent and its
344 enzymatic accessibility reported in the literature seems ambiguous. For example, Blayo et al. (2016)
345 reported that the best proteolysis efficiency of β-lactoglobulin was obtained in the case of the less
346 denaturing treatments caused by thermal treatment (75 ºC, pH 7.0). However, Belloque et al. (2007)

347 found that proteolysis efficiency of β-lactoglobulin was markedly improved when the protein was
348 extensively denatured after high-pressure treatment (300 MPa, pH 2.5). This discrepancy may be due
349 to the fact that compared to the thermal treatment, the protein denaturation caused by high-pressure
350 treatment at pH 2.5 would result in the formation of protein aggregates with different structural
351 characteristics (Belloque et al., 2007; Blayo et al., 2016).

352 The intrinsic fluorescence emission spectrum, excited at 290 nm, is mainly produced by
353 tryptophan (Trp) residues in proteins, and they are very sensitive to their micro-environment. It is
354 generally recognized that the intrinsic fluorescence emission maximum (λ_{max}) suffers a red shift when
355 the Trp chromophores become more exposed to the hydrophilic medium (Pallarès, Vendrell, Avilès,
356 & Ventura, 2004). As shown in **Fig. 4**, the fluorescence emission spectrum of untreated PPI showed
357 a λ_{max} at around 324 nm, which was a typical fluorescence profile of Trp residues located in a
358 hydrophobic environment, such as the interior of globulins (Choi, Kim, Park, & Moon, 2005). In
359 addition, the spectrum showed a second superimposed peak at a wavelength of approximately 331
360 nm. This shoulder peak could be attributed to the presence of some Trp exposed to the solvent. By
361 contrast, the λ_{max} of S-PPI and TS-PPI shifted to higher wavelength (red-shift), indicating an increased
362 exposure of the Trp residues to the aqueous solvent. Compared to S-PPI, TS-PPI showed a higher
363 λ_{max} (around 339 nm) and fluorescence intensity. Since the nature of the environment of Trp
364 chromophores in proteins mainly depends on their molecular flexibility (Beck, Knoerzer, & Arcot,
365 2017; Choi et al., 2005; Pallarès et al., 2004), this observation suggests that the protein conformation
366 in TS-PPI was more unfolded than that in S-PPI and was therefore more easily accessible to proteases.

367 FTIR spectroscopy is especially useful for determining the secondary structures of proteins in
368 aqueous solution. Attention is usually devoted to the amide I region (1600–1700 cm^{-1}) of IR spectra,

369 because the amide I vibration of polypeptide chain is very sensitive to the alterations of secondary
370 structures (Byler & Susi, 1986; Lefèvre & Subirade, 2000). **Fig. 5** shows the second derivative FTIR
371 spectra of untreated PPI, S-PPI and TS-PPI. It is observed that the amide I spectrum of untreated PPI
372 contained 6 major adsorption bands. Based on previous studies (Baltacıoğlu et al., 2017; Beck et al.,
373 2017; Byler & Susi, 1986; Kong & Yu, 2007; Lefèvre & Subirade, 2000), these bands were assigned,
374 and their compositions were calculated **(**see **Table 5)**. The secondary structure composition of the
375 untreated PPI prepared in our lab is similar with those of laboratory-prepared PPI predicted by other
376 researchers, which shows that native peanut proteins contained high proportion of α-helix (1659 cm^{-}
377 ^{1}, 34.9%) and intramolecular β-sheet (1631 cm^{-1}, 31.7%) structures (Ochoa-Rivas et al., 2017). In
378 addition, the band located at 1618 cm^{-1} was characteristic of intermolecular β-sheet structures
379 attributed to the association of globular proteins (i.e., spherical protein aggregates), and the presence
380 of the band at 1682 cm^{-1} suggested that they consisted in anti-parallel β-sheet (Byler & Susi, 1986;
381 Kong & Yu, 2007; Lefèvre & Subirade, 2000; Zou, Li, Hao, Hu, & Ma, 2013). After sonication
382 treatment alone, the components of native-like secondary structures in S-PPI decreased, but still
383 retained a high proportion. Concomitantly, the intensity of the components attributed to
384 intermolecular β-sheet located at 1618 cm^{-1} and 1682 cm^{-1} both increased markedly. It may be that
385 during sonication treatment, some parts of the hydrogen bonds stabilizing the native secondary
386 structures of peanut proteins were disrupted, causing the partial denaturation and unfolding of protein
387 molecules. Due to the increased attractive force (e.g., hydrophobic interaction) after unfolding, the
388 partly denatured peanut protein molecules associated to constitute spherical protein aggregates
389 through anti-parallel intermolecular β-sheet. In fact, this finding may explain why sonication alone
390 could only cause a limited improvement on the enzymatic accessibility of S-PPI, because spherical

protein aggregates still bore compact globular structures that were resistant to enzymatic proteolysis (Belloque et al., 2007; Nyemb et al., 2014). In addition, it is noteworthy that near the original intermolecular β-sheet (1618 cm^{-1}), the spectrum of S-PPI showed a new superimposed band at 1621 cm^{-1}, suggesting the formation of new intermolecular β-sheet (Byler & Susi, 1986; Lefèvre & Subirade, 2000; Zou et al., 2013).

In contrast, from the FTIR spectrum of TS-PPI, it is observed that after thermosonication, the majority of the native-like secondary structures of peanut proteins was lost, and the content of random coil structure was increased. This observation is consistent with the DSC measurements and confirms that heat could present a markedly additive effect to ultrasound on denaturing peanut proteins. This may be due to the fact that after optimizing the operating conditions, the combined use of heat and ultrasound could produce a more intense and uniform acoustic cavitation field than ultrasound alone did (Patist & Bates, 2008; Villamiel & de Jong, 2000). As a result, most of the regular secondary structures of peanut proteins were disrupted by acoustic cavitation, causing the extensive denaturation and unfolding of protein molecules. On the other hand, compared to S-PPI, the new intermolecular β-sheet in TS-PPI shifted from 1621 cm^{-1} to 1622 cm^{-1} and showed a marked increase in intensity; however, the original intermolecular β-sheet at 1618 cm^{-1} and that represented anti-parallel β-sheet at 1682 cm^{-1} both showed a decrease in intensity. Based on these observations, it can be inferred that the new protein aggregates formed in TS-PPI were predominantly associated by parallel intermolecular β-sheets. The β-sheet structures, which are essential in the formation of protein aggregates by acting as junction zones, play a crucial role in determining the structures and properties of protein aggregates (Kong & Yu, 2007; Lefèvre & Subirade, 2000). According to the literature, during protein aggregation caused by heating (Zou et al., 2013), by ultrasound (Chan et al., 2005; Stathopulos et al., 2004), or by high pressure

(Torrent et al., 2004), the appearance of high proportion of parallel intermolecular β-sheets is usually a strong evidence that fibril protein aggregates are being formed.

In order to confirm the formation of fibril protein aggregates in TS-PPI, thioflavin-T (ThT) fluorescence assay was performed, which is a commonly used method in the detection of fibrils formation (Biancalana & Koide, 2010; Stathopulos et al., 2004). When ThT binds to flat β-sheet surface, such as those in fibrils, the dye displays an enhanced fluorescence (Biancalana & Koide, 2010). From **Fig. 6**, it is seen that both the untreated PPI and S-PPI showed a small ThT fluorescent intensity, suggesting that there was little fibril protein structure presented in the original peanut proteins. In contrast, TS-PPI showed a dramatically enhanced ThT fluorescence, with a maximum signal appearing at approximately 480 nm. These results are consistent with the FTIR measurements and provide confirmation that fibril protein aggregates were formed in TS-PPI. It should be noted that compared to native globular proteins or spherical protein aggregates, fibril protein aggregates have been proven to be more flexible and provide easier access to protease (Belloque et al., 2007; Nyemb et al., 2014). Therefore, this finding might explain the much increased enzymatic accessibility of TS-PPI relative to that of untreated PPI or S-PPI.

To summarize, this study demonstrated that after optimizing the treatment conditons using RSM, thermosonication could be more effective than sonication in enhancing the enzymatic proteolysis of PPI. After thermosonication pre-treatment (475.0 W, 72 °C), the enzymatic accessibility of the major proteolysis-resistant globulin arachin in PPI was substantially improved, which made the enzymatic proteolysis of TS-PPI not only intensive (higher DH), but also extensive (higher PS). The TS-PPIH prepared in the current study was mainly composed of peptides with MW < 20 kDa and showed a PS of 93.5%, much higher than those of untreated PPI (PS = 74.8%), PPIH or S-PPIH. It was found that

heat could present a markedly additive effect to ultrasound on denaturing peanut proteins, probably because the acoustic cavitation activity generated by ultrasound was closely related to the temperature of sonicated medium. Unlike partially unfolded proteins, the extensively unfolded proteins allowed a structural rearrangement of polypeptide chains. TS-PPI had a high proportion of parallel intermolecular β-sheets and displayed a dramatically enhanced ThT fluorescence, suggesting that the structural modifications (unfolding and aggregation) induced by thermosonication probably resulted in the formation of fibril protein aggregates in TS-PPI rather than spherical protein aggregates normally formed in S-PPI. As a result, the protein conformation of TS-PPI appeared to be more unfolded and flexible than that of untreated PPI or S-PPI, and therefore was more easily accessible to protease. Based on these findings and considering that thermosonication only need a mild temperature requirement that will not cause a significant increase in economic cost, it is encouraging to conclude that thermosonication pre-treatment could be a highly effective and feasible technique to improve the enzymatic accessibility of globular proteins, producing prominent functional benefits for the protein hydrolysates. However, further studies are needed to elucidate more clearly the details of the mechanisms involved in thermosonication-induced protein unfolding and aggregation.

Acknowledgement

We are grateful for the financial support from National Natural Science Foundation of China (No. 31601416) and Guangdong Provincial Science and Technology Project (No. 2016A020210113 and 2017A020208064). LC acknowledges the financial support from the School of Chemical Engineering and Light Industry for his studies in the University of Leeds.

References

Adler-Nissen, J. (1986). *Enzymatic Hydrolysis of Food Proteins*. London, UK: Applied Science Publishers.

Ashokkumar, M., Lee, J., Kentish, S., & Grieser, F. (2007). Bubbles in an acoustic field: an overview. *Ultrasonic Sonochemistry, 14*(4), 470–475.

Baltacıoğlu, H., Bayındırl, A., & Severcan, F. (2017). Secondary structure and conformational change of mushroom polyphenol oxidase during thermosonication treatment by using FTIR spectroscopy. *Food Chemistry, 214*, 507–514.

Bax, M. L., Aubry, L., Ferreira, C., Daudin, J. D., Gatellier, P., & Rémond, D., et al. (2012). Cooking temperature is a key determinant of in vitro meat protein digestion rate: investigation of underlying mechanisms. *Journal of Agricultural and Food Chemistry, 60*(10), 2569–2576.

Beck, S. M., Knoerzer, K., & Arcot, J. (2017). Effect of low moisture extrusion on a pea protein isolate's expansion, solubility, molecular weight distribution and secondary structure as determined by Fourier Transform Infrared Spectroscopy (FTIR). *Journal of Food Engineering, 214*, 166–174.

Belloque, J., Chicón, R., & López-Fandiño, R. (2007). Unfolding and refolding of beta-lactoglobulin subjected to high hydrostatic pressure at different pH values and temperatures and its influence on proteolysis. *Journal of Agricultural and Food Chemistry, 55*(13), 5282–5288.

Biancalana, M., & Koide, S. (2010). Molecular mechanism of thioflavin-T binding to amyloids fibrils. *Biochimica et Biophysica Acta, 1804*, 1405–1412.

Blayo, C., Vidcoq, O., Lazennec, F., & Dumay, E. (2016). Effects of high pressure processing (hydrostatic high pressure and ultra-high pressure homogenisation) on whey protein native state

and susceptibility to tryptic hydrolysis at atmospheric pressure. *Food Research International, 79*, 40–53.

Byler, D. M., & Susi, H. (1986). Examination of the secondary structure of proteins by deconvolved FTIR spectra. *Biopolymers*, *25*(3), 469–487.

Chan, J. C. C., Oyler, N. A., Yau, W. M., & Tycko, R. (2005). Parallel beta-sheets and polar zippers in amyloid fibrils formed by residues 10-39 of the yeast prion protein Ure2p. *Biochemistry*, *44*(31), 10669–10680.

Chandrapala, J., Oliver, C., Kentish, S., & Ashokkumar, M. (2012). Ultrasonics in food processing. *Ultrasonics Sonochemistry, 19*(5), 975–983.

Chen, L., Chen, J. S., Yu, L., & Wu, K. G. (2016). Improved emulsifying capabilities of hydrolysates of soy protein isolate pretreated with high pressure microfluidization. *LWT-Food Science and Technology, 69*, 1–8.

Chen, L., Chen, J. S., Yu, L., Wu, K. G., & Zhao, M. M. (2018). Emulsification performance and interfacial properties of enzymically hydrolyzed peanut protein isolate pretreated by extrusion cooking. *Food Hydrocolloids, 77*, 607–616.

Choi, S. J., Kim, H. J., Park, K. H., & Moon, T. W. (2005). Molecular characteristics of ovalbumin-dextran conjugates formed through the Maillard reaction. *Food Chemistry, 92*(1), 93–99.

Colombo, A., Ribtta, P. D., & León, A. E. (2010). Differential scanning calorimetry (DSC) studies on the thermal properties of peanut proteins. *Journal of Agricultural and Food Chemistry, 58*(7), 4434–4439.

Ghatak, S. K., & Sen, K. (2013). Peanut proteins: Application, aliments and possible remediation. *Journal of Industrial and Engineering Chemistry, 19*(2), 369–374.

Gordon, L., & Pilosof, Ana M. R. (2010). Application of high-intensity ultrasounds to control the size of whey proteins particles. *Food Biophysics, 5*(3), 203–210.

Jamdar, S. N., Rajalakshmi, V., Pednekar, M. D., Juan, F., Yardi, V., & Sharma, A. (2010). Influence of degree of hydrolysis on functional properties, antioxidant activity and ACE inhibitory activity of peanut protein hydrolysate. *Food Chemistry, 121*(1), 178–184.

Jiang, S. S., Ding, J. Z., Andrade, J., Rababah, T. M., Almajwal, A., & Abulmeaty, M. M., et al. (2017). Modifying the physicochemical properties of pea protein by pH-shifting and ultrasound combined treatments. *Ultrasonics-Sonochemistry, 38*, 835–842.

Kong, J. L., & Yu, S. N. (2007). Fourier transform infrared spectroscopic analysis of protein secondary structures. *Acta Biochimica et Biophysica Sinica, 39*(8), 549–559.

Laemmli, U. K. (1970). Cleavage of structural proteins during assembly of head of bacteriophage-T4. *Nature, 227*(5259), 680–685.

Lefèvre, T., & Subirade, M. (2000). Molecular Differences in the formation and structure of fine-stranded and particulate *β*-lactoglobulin gels. *Biopolymers, 54*(7), 578–586.

Li, H., Prairie, N., Udenigwe, C. C., Adebiyi, A. P., Tappia, P. S., & Aukema, H. M., et al. (2011). Blood pressure lowering effect of a pea protein hydrolysate in hypertensive rats and humans. *Journal of Agricultural and Food Chemistry, 59*(18), 9854–9860.

Nyemb, K., Guérin-Dubiard, C., Dupont, D., Jardin, J., Rutherfurd, S. M., & Nau, F. (2014). The extent of ovalbumin *in vitro* digestion and the nature of generated peptides are modulated by the morphology of protein aggregates. *Food Chemistry, 157*, 429–438.

Ochoa-Rivas, A., Nava-Valdez, Y., Serna-Saldívar, S. O., & Chuck-Hernández, C. (2017). Microwave and ultrasound to enhance protein extraction from peanut flour under alkaline

conditions: effects in yield and functional properties of protein isolates. *Food and Bioprocess Technology, 10*(3), 543–555.

Pallarès, I., Vendrell, J., Avilès, F. X., & Ventura, S. (2004). Amyloid fibril formation by a partially structured intermediate state of α-chymotrypsin. *Journal of Molecular Biology, 342*(1), 321–331.

Patist, A., & Bates, D. (2008). Ultrasonic innovations in the food industry: From the laboratory to commercial production. *Innovative Food Science & Emerging Technologies, 9*(2), 147–154.

Perrot, C., Quillien, L., & Guéguen, J. (1999). Identification by immunoblotting of pea (*Pisum sativum* L.) proteins resistant to in vitro enzymatic hydrolysis. *Sciences Des Aliments, 19*(3–4), 377–390.

Ribeiro, M. D., Valdramidis, V. P., Nunes, C. A., & de Souza, V. R. (2017). Synergistic effect of thermosonication to reduce enzymatic activity in coconut water. *Innovative Food Science & Emerging Technologies, 41*, 404–410.

Stathopulos, P. B., Scholz, G. A., Hwang, Y. M., Rumfeldt, J. A. O., Lepock, J. R., & Meiering, E. M. (2004). Sonication of proteins causes formation of aggregates that resemble amyloid. *Protein Science, 13*(11), 3017–3027.

Sun, M. J., Mu, T. H., Sun, H. N., & Zhao, M. (2014). Digestibility and structural properties of thermal and high hydrostatic pressure treated sweet potato (*Ipomoea batatas* L.) protein. *Plant Foods for Human Nutrition, 69*(3), 270–275.

Tavano, O. L. (2013). Protein hydrolysis using proteases: An important tool for food biotechnology. *Journal of Molecular Catalysis B: Enzymatic, 90*, 1–11.

Torrent, J., Alvarez-Martinez, M. T., Herricane, M. C., Heitz, F., Liautard, J. P., & Balny, C., et al. (2004). High pressure induces scrapie-like prion protein misfolding and amyloid fibril formation. *Biochemistry, 43*(22), 7162–7170.

Villamiel, M., & de Jong, P. (2000). Influence of high-intensity ultrasound and heat treatment in continuous flow on fat, proteins, and native enzymes of milk. *Journal of Agricultural and Food Chemistry, 48*(2), 472–478.

Zeeb, B., McClements, D. J., & Weiss, J. (2017). Enzyme-based strategies for structuring foods for improved functionality. *Annual Review of Food Science and Technology, 8*, 21–34.

Zhao, G. L., Liu, Y., Zhao, M. M., Ren, J. Y., & Yang, B. (2011). Enzymatic hydrolysis and their effects on conformational and functional properties of peanut protein isolate. *Food Chemistry, 127*, 1438–1443.

Zhao, X. Y., Chen, J., & Du, F. L. (2012). Potential use of peanut by-products in food processing: a review. *Journal of Food Science and Technology, 49*(5), 521–529.

Zou, Y., Li, Y. Y., Hao, W. Y., Hu, X. Q., & Ma, G. (2013). Parallel *β*-sheet fibril and antiparallel *β*-sheet oligomer: new insights into amyloid formation of hen egg white lysozyme under heat and acidic condition from FTIR spectroscopy. *Journal of Physical Chemistry B, 117*(15), 4003-4013.

560 **Legends**

561 **Table 1.** Coded settings for the process parameters of thermosonication pre-treatment, according to
562 a central composite design.

563 **Table 2.** Experimental design used in the response surface methodology studies and the response.

564 **Table 3.** Analysis of variance for the response surface quadratic model for the DH of TS-PPIH

565 **Table 4.** Denaturation Temperature (T_d), denaturation enthalpy (ΔH), degree of hydrolysis (DH), and
566 protein solubility (PS) of different protein samples*

567 **Table 5.** FTIR band positions and secondary structure assignments of untreated PPI, S-PPI and TS-
568 PPI*

569 **Fig. 1.** 3D response surface graph (a) and binary contour plot (b) for the effects of power-output and
570 temperature of thermosonication pre-treatment on the DH of TS-PPIH.

571 **Fig. 2.** SDS-PAGE profiles of different protein samples and their hydrolysates prepared with
572 pancreatin-induced proteolysis. S66: conarachin; S41, S40, and S38: acidic subunits of arachin; S27:
573 basic subunits of arachin; M, molecular weight marker.

574 **Fig. 3.** DSC thermograms of different protein samples in 0.01 mol/L phosphate buffer (100 g/L, pH
575 7.0).

576 **Fig. 4.** Intrinsic emission fluorescence spectra of untreated PPI, S-PPI and TS-PPI in 0.01 mol/L
577 phosphate buffer (15g /L, pH 7.0).

578 **Fig. 5.** Second derivative FTIR spectra of untreated PPI, S-PPI and TS-PPI in 0.01 mol/L D_2O
579 phosphate buffer (50 g/L, pH 7.0).

580 **Fig. 6.** Normalized thioflavin-T fluorescence intensity of untreated PPI, S-PPI and TS-PPI in 0.01
581 mol/L phosphate buffer (0.2 g /L, pH 7.0).

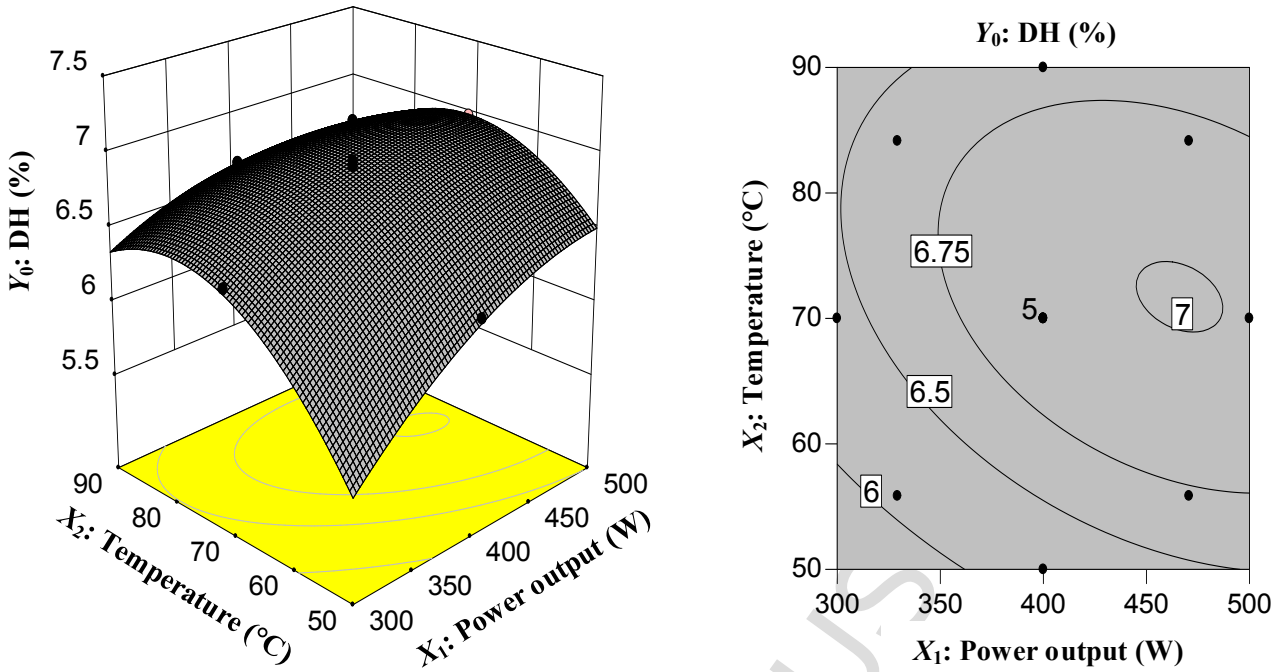

a: 3D graph b: Binary contour plot

Fig. 1.

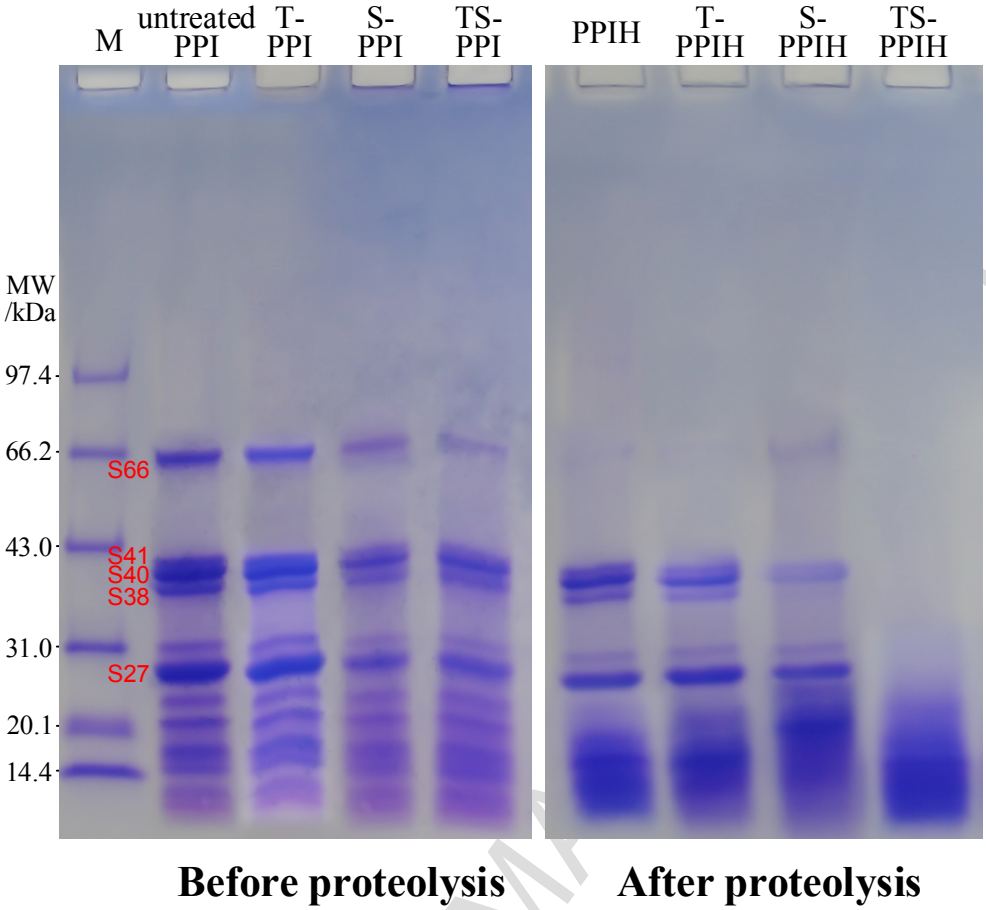

Fig. 2.

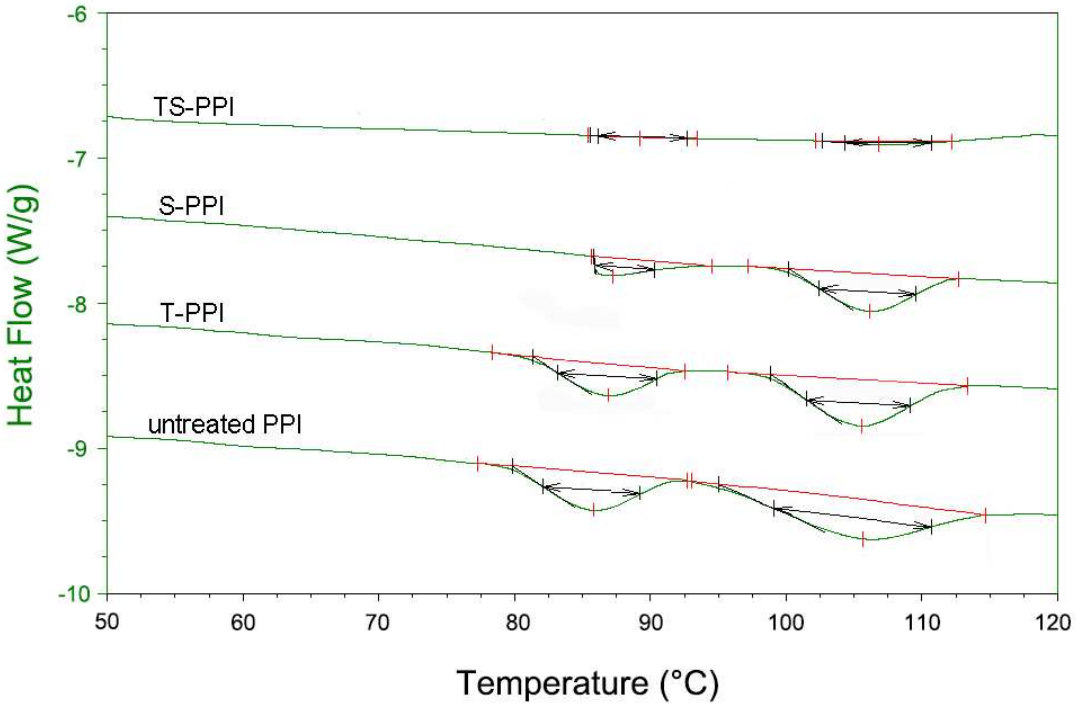

Fig. 3.

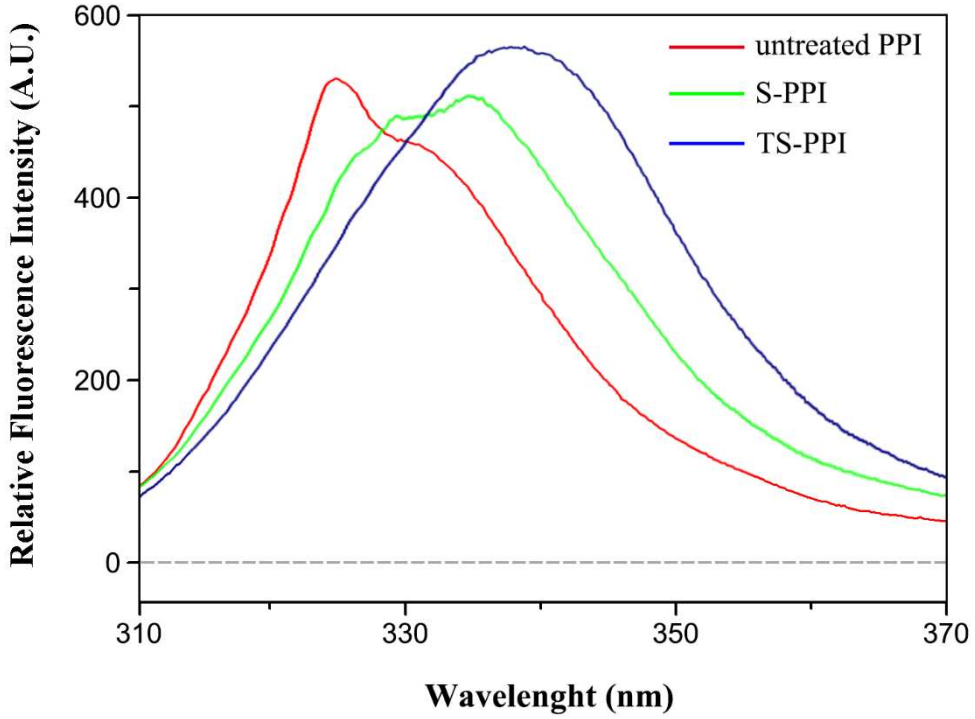

Fig. 4.

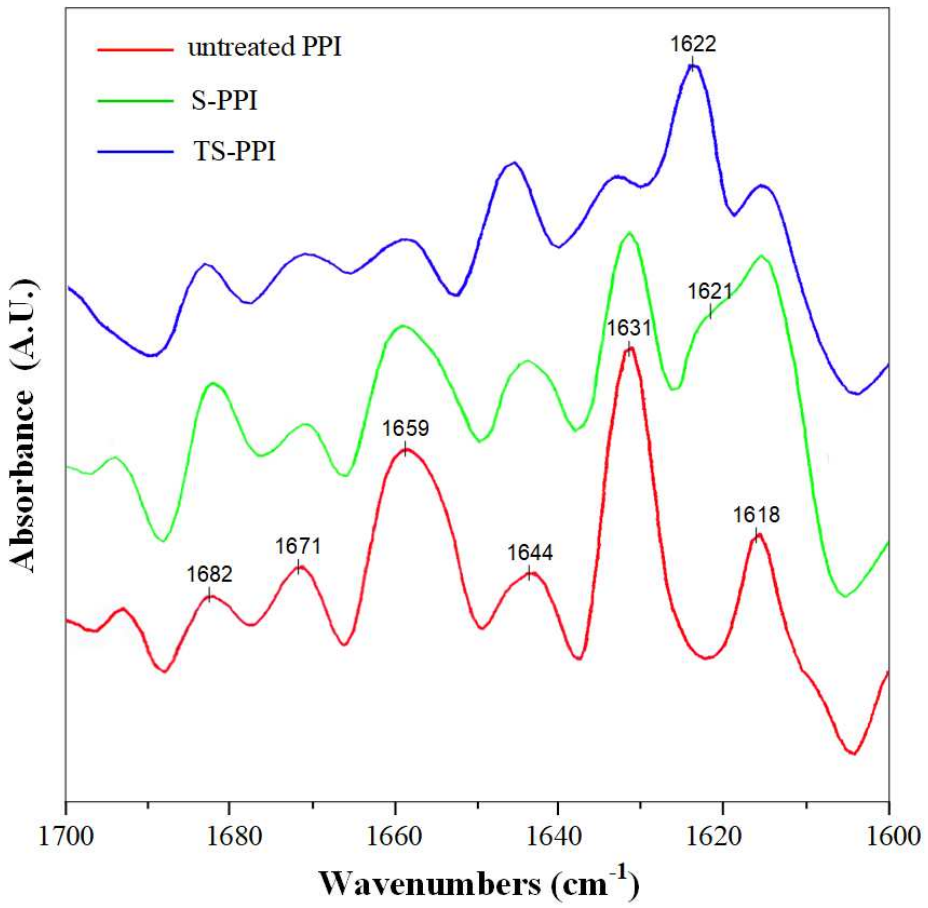

Fig. 5.

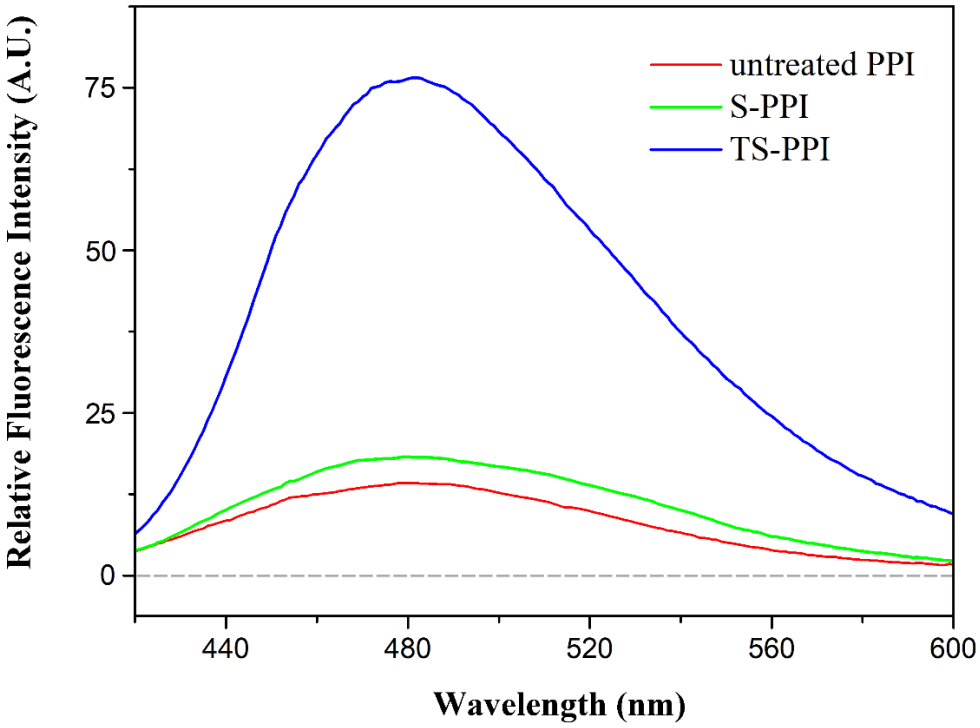

Fig. 6.

Highlights

"Improved enzymatic accessibility of peanut protein isolate pre-treated using thermosonication"

by Chen *et al*.

Food Hydrocolloids.

- Thermosonication could be more effective than sonication in improving the enzymatic accessibility of peanut protein isolate (PPI).
- Hydrolysates of thermosonicated PPI (TS-PPI) showed a high protein solubility of ~90%.
- Heat could present a markedly additive effect to ultrasound on denaturing peanut proteins.
- Fibril protein aggregates were found in TS-PPI
- Protein conformation of TS-PPI was more unfolded and flexible than that of sonicated PPI.

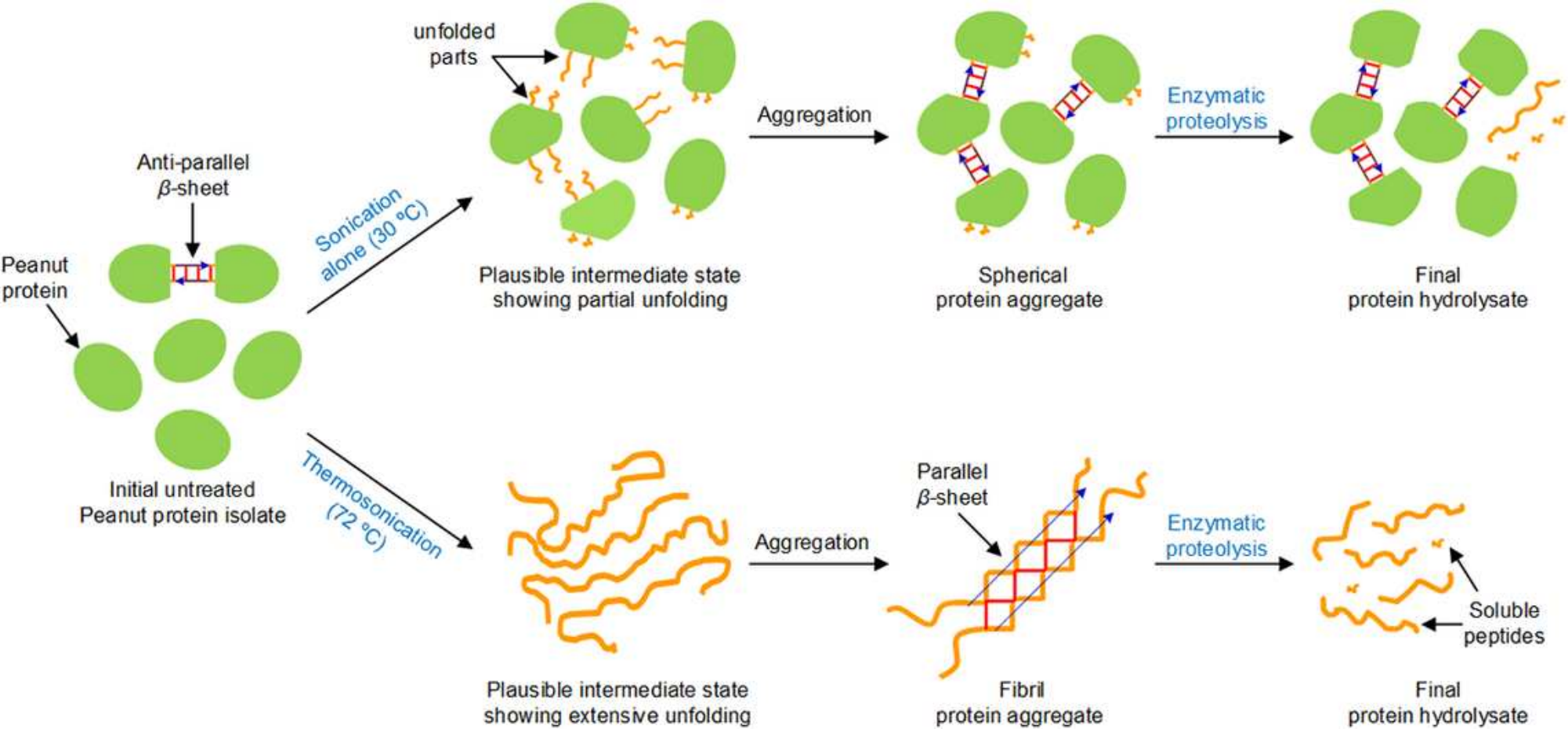
unfolded parts
Anti-parallel β-sheet
Peanut protein
Sonication alone (30 °C)
Aggregation
Enzymatic proteolysis
Plausible intermediate state showing partial unfolding
Spherical protein aggregate
Final protein hydrolysate
Initial untreated Peanut protein isolate
Thermosonication (72 °C)
Aggregation
Parallel β-sheet
Enzymatic proteolysis
Soluble peptides
Plausible intermediate state showing extensive unfolding
Fibril protein aggregate
Final protein hydrolysate

Table 1. Coded settings for the process parameters of thermosonication pre-treatment, according to a central composite design.

Independent variables	Symbol	Levels				
		–1.414	–1	0	1	1.414
Power-output (W)	X_1	300	329.3	400	470.7	500
Temperature (ºC)	X_2	50	55.9	70	84.1	90

Table 2. Experimental design used in the response surface methodology studies and the response.

Experriment	Coded levels of variable		DH (Y_0, %)	
	Power-output (X_1, W)	Temperature (X_2, ºC)	Experimental	Predicted
1	400 (0)	70 (0)	6.91	6.90
2	400	70	6.95	6.90
3	470.7 (1)	55.9 (–1)	6.71	6.72
4	329.3 (–1)	55.9	6.06	6.10
5	400	70	6.85	6.90
6	400	70	6.92	6.90
7	400	70	6.88	6.90
8	329.3	84.1 (1)	6.58	6.61
9	470.7	84.1	6.83	6.82
10	400	50 (–1.414)	6.25	6.22
11	500 (1.414)	70	6.98	6.99
12	400	90 (1.414)	6.65	6.65
13	300 (–1.414)	70	6.44	6.40

Table 3. Analysis of variance for the response surface quadratic model for the DH of TS-PPIH

Source of variance	Degree of freedom	Sum of squares	Mean square	*F*-value	*p*-value
Model	5	0.99	0.20	122.18	< 0.0001
Linear					
X_1	1	0.35	0.35	213.50	< 0.0001
X_2	1	0.18	0.18	112.13	< 0.0001
Interaction					
X_1X_2	1	0.040	0.040	24.68	0.0016
Quadratic					
X_1^2	1	0.076	0.076	47.10	0.0002
X_2^2	1	0.42	0.42	104.57	< 0.0001
Statistic analysis for the model					
Lack of fit	3	0.0055	0.0018	1.24	0.4058
$R^2 = 0.9887$		adjusted-$R^2 = 0.9806$		predicted -$R^2 = 0.9520$	

Table 4. Denaturation Temperature (T_d), denaturation enthalpy (ΔH), degree of hydrolysis (DH), and protein solubility (PS) of different protein samples*

Samples	Conarachin		Arachin		DH (%)		PS (%)	
	T_{d1} (°C)	ΔH_1 (J/g)	T_{d2} (°C)	ΔH_2 (J/g)	Before Proteolysis	After Proteolysis	Before Proteolysis	After Proteolysis
PPI	85.9 (±0.12) [c]	5.2 (±0.06) [a]	105.3 (±0.15) [c]	6.3 (±0.17) [a]	--	2.68 (±0.05) [c]	74.8 (±0.3) [e]	77.5 (±0.3) [d]
T-PPI	87.1 (±0.16) [b]	4.9 (±0.13) [b]	105.2 (±0.09) [c]	5.8 (±0.12) [b]	0.12 (±0.02) [e]	2.73 (±0.08) [c]	75.2 (±0.4) [e]	82.1 (±0.6) [c]
S-PPI	87.5 (±0.23) [b]	1.3 (±0.07) [c]	106.1 (±0.17) [b]	5.5 (±0.14) [c]	0.19 (±0.03) [d]	3.84 (±0.12) [b]	73.6 (±0.5) [f]	86.2 (±0.5) [b]
TS-PPI	89.2 (±0.15) [a]	0.2 (±0.05) [d]	107.4 (±0.11) [a]	0.6 (±0.10) [d]	0.27 (±0.03) [d]	7.16 (±0.09) [a]	60.9 (±0.4) [g]	93.5 (±0.4) [a]

* In the comparison of the same type of index, results having different letters are significantly different ($p<0.05$).

Table 5. FTIR band positions and secondary structure assignments of untreated PPI, S-PPI and TS-PPI*

Samples	Band position (cm^{-1})	Assignment	Band area (%)
untreated PPI	1618, 1682	Anti-parallel intermolecular β-sheets	13.5 (±0.3) [c]
	1631	Intramolecular β-sheets	31.7 (±0.5) [b]
	1644	Random coil	10.3 (±0.3) [d]
	1659	α-helix	34.9 (±0.4) [a]
	1671	β-turn	9.6 (±0.2) [e]
S-PPI	1618, 1682	Anti-parallel intermolecular β-sheets	23.8 (±0.6) [b]
	1621	Intermolecular β-sheets	9.7 (±0.2) [e]
	1631	Intramolecular β-sheets	20.3 (±0.4) [c]
	1645	Random coil	12.8 (±0.5) [d]
	1660	α-helix	26.1 (±0.5) [a]
	1671	β-turn	7.3 (±0.3) [f]
TS-PPI	1618, 1682	Anti-parallel intermolecular β-sheets	14.1 (±0.4) [c]
	1622	Parallel intermolecular β-sheets	31.6 (±0.3) [a]
	1632	Intramolecular β-sheets	13.3 (±0.2) [d]
	1646	Random coil	24.2 (±0.4) [b]
	1659	α-helix	9.0 (±0.2) [e]
	1671	β-turn	7.8 (±0.3) [f]

* In the comparison of the band area for each sample, results having different letters are significantly different ($p<0.05$).